



## Sine-Gordon 2-pi-kink dynamics in the presence of small perturbations

Olsen, O. H.; Samuelsen, Mogens Rugholm

*Published in:*  
Physical Review B

*Link to article, DOI:*  
[10.1103/PhysRevB.28.210](https://doi.org/10.1103/PhysRevB.28.210)

*Publication date:*  
1983

*Document Version*  
Publisher's PDF, also known as Version of record

[Link back to DTU Orbit](#)

*Citation (APA):*  
Olsen, O. H., & Samuelsen, M. R. (1983). Sine-Gordon 2-pi-kink dynamics in the presence of small perturbations. *Physical Review B*, 28(1), 210-217. <https://doi.org/10.1103/PhysRevB.28.210>

---

### General rights

Copyright and moral rights for the publications made accessible in the public portal are retained by the authors and/or other copyright owners and it is a condition of accessing publications that users recognise and abide by the legal requirements associated with these rights.

- Users may download and print one copy of any publication from the public portal for the purpose of private study or research.
- You may not further distribute the material or use it for any profit-making activity or commercial gain
- You may freely distribute the URL identifying the publication in the public portal

If you believe that this document breaches copyright please contact us providing details, and we will remove access to the work immediately and investigate your claim.

Sine-Gordon  $2\pi$ -kink dynamics in the presence of small perturbations

O. H. Olsen

*NIRO Atomizer, Research and Development System and Design Division, Gladsaxevej,  
DK-2860 Soeborg, Denmark*

M. R. Samuelsen

*Physics Laboratory I, The Technical University of Denmark, DK-2800 Lyngby, Denmark*

(Received 3 June 1982; revised manuscript received 23 November 1982)

The influence of external driving forces on the  $2\pi$ -kink solution to the sine-Gordon equation is examined. The analysis is based on the approach that the solution to the problem can be divided into a  $2\pi$ -kink part and a background or vacuum part. The behavior of the  $2\pi$  kink depends strongly on the initial state of the vacuum. Excellent agreement between the analysis and numerical solution of representative initial-value problems is found.

## I. INTRODUCTION

Nonlinear solitary waves are currently being used in a remarkable variety of contexts in almost every area of physics. In particular, the sine-Gordon  $2\pi$ -kink solution is ubiquitous in its application as a model for, e.g., dislocations in crystals, domain walls in ferromagnets, and propagation of flux quanta, fluxons, in Josephson transmission lines.

Recently the influence of the presence of external driving forces on the  $2\pi$ -kink solution has attracted considerable interest.<sup>1</sup> In contrast to prevalent results<sup>2,3</sup> it was found that the  $2\pi$  kink does not behave like a Newtonian particle in a conservative force field. In Ref. 4 it was shown that the vacuum "motion," i.e., the behavior of solutions at  $x = \pm \infty$  affects the motion of the  $2\pi$  kink. The non-Newtonian behavior of the  $2\pi$  kink<sup>1</sup> is observed when the vacuum is in an excited state, while a Newtonian behavior of the  $2\pi$  kink is observed<sup>5,6</sup> if the vacuum is in the ground state.

Our method is to divide the solution into two parts, a homogeneous part  $\phi^{\text{vac}}(t)$ , which is the solution at  $x = \pm \infty$ , and a  $2\pi$ -kink part, which contains all the  $k \neq 0$  parts of the possible radiation.

The  $k = 0$  part of the radiation is contained in  $\phi^{\text{vac}}(t)$ . For the momentum connected to the  $2\pi$ -kink part  $P_k$  an equation of motion is derived without any approximations. For some physical applications it is sufficient to know the  $2\pi$ -kink momentum,<sup>7</sup> and then the method yields exact results even for large perturbations.<sup>7</sup> Our basic approximation for determining the  $2\pi$ -kink motion is to replace the momentum  $P_k$  by the small perturbation result<sup>3</sup>  $8\gamma(v)v$ ,  $v$  being the  $2\pi$ -kink velocity.

The influence on a  $2\pi$  kink of the initial state of the vacuum,  $\phi^{\text{vac}}(0)$  and  $\dot{\phi}_t^{\text{vac}}(0)$ , the external driving

force, and the dissipation are investigated in detail. The investigation includes, in addition to the perturbation analysis of the  $2\pi$  kink, a numerical solution of corresponding initial-value problems. Good agreement between the perturbation results and the numerical results is found also for large  $t$  and also for velocities *not* fulfilling the condition  $v \ll 1$ . The initial state of the vacuum influences the velocity and trajectory of the  $2\pi$  kink for the  $t \leq 5$ , while for larger times the influence decreases. Furthermore, we find that for  $\eta \geq 0.5$  the behavior of the  $2\pi$  kink depends strongly on the initial state of the vacuum.

The main difference between our treatment and the works referred to lies merely in the initial state of the vacuum. The method used in Refs. 1 and 2 is based on the pure sine-Gordon soliton and therefore is restricted to the case  $\phi^{\text{vac}}(0) = \dot{\phi}_t^{\text{vac}}(0) = 0$  and to small  $t$  and small velocities. On the other hand, this method enables one to calculate the full radiation spectrum.<sup>1</sup> The results of Ref. 3 agree with ours under the tacit assumption that  $\dot{\phi}_t^{\text{vac}}(t) = 0$ .

The outline of the paper is as follows: In Sec. II we obtain an equation for the time dependence of the momentum of the  $2\pi$  kink. Expressions for the acceleration and the velocity are then calculated. Furthermore, we examine the influence of a time-varying force term. In Sec. III we solve the corresponding initial-value problems numerically and illustrate the influence of the initial state of the vacuum and the force term. Section IV contains a comparison between the numerical results and the perturbation theory. Finally, in Sec. V we summarize and conclude.

II. TIME EVOLUTION OF THE  $2\pi$  KINK

The equation in question is the perturbed sine-Gordon equation

$$\phi_{xx} - \phi_{tt} - \sin\phi = \eta + \alpha\phi_t, \quad (2.1)$$

where the right-hand side represents the perturbation, the first term being the constant "force," and the second term the dissipation. A single  $2\pi$ -kink solution to Eq. (2.1),  $\phi(x, t)$ , must fulfill the condition  $\phi(+\infty, t) - \phi(-\infty, t) = 2\pi$ . Furthermore, the  $2\pi$  kink is localized. Therefore it is convenient to divide  $\phi(x, t)$  into a pure  $2\pi$ -kink part  $\phi^k(x, t)$ , where  $\phi^k(\pm\infty, t) = 0 \bmod 2\pi$ , and a background (vacuum) part  $\phi^{\text{vac}}(t)$  only depending on time:

$$\phi(x, t) = \phi^k(x, t) + \phi^{\text{vac}}(t). \quad (2.2)$$

The vacuum part alone must satisfy Eq. (2.1), i.e., the pendulum equation,

$$\phi_{tt}^{\text{vac}} + \alpha\phi_t^{\text{vac}} + \sin\phi^{\text{vac}} + \eta = 0. \quad (2.3)$$

The idea behind the splitting of  $\phi(x, t)$  in Eq. (2.2) is to take out the homogeneous part that would be there even without the presence of a  $2\pi$  kink.

The easiest way to derive the equation of motion for the  $2\pi$  kink is to calculate the *total* momentum  $P$ ,

$$\begin{aligned} P &= \int -\phi_x \phi_t dx = \int -\phi_x^k \phi_t^k dx - 2\pi\phi_t^{\text{vac}}(t) \\ &= P_k - 2\pi\phi_t^{\text{vac}}(t), \end{aligned} \quad (2.4)$$

where  $P_k$  is the  $2\pi$ -kink contribution to the momentum. Taking the time derivative of  $P$  and using the equation of evolution for  $\phi$ , Eq. (2.1), we get

$$\frac{dP}{dt} = -\alpha P + 2\pi\eta, \quad (2.5)$$

the equation of motion for the *total* momentum  $P$ . Inserting Eq. (2.4) into Eq. (2.5), we finally arrive at

$$\frac{dP_k}{dt} = -\alpha P_k + 2\pi(\eta + \alpha\phi_t^{\text{vac}} + \phi_{tt}^{\text{vac}}) \quad (2.6)$$

$$= -\alpha P_k - 2\pi \sin[\phi^{\text{vac}}(t)], \quad (2.7)$$

which is the equation of motion for the momentum of the  $2\pi$  kink. In the last step we have used Eq. (2.3) on  $\phi^{\text{vac}}(t)$ . It should be emphasized that until now *no* approximation has been made and that  $\eta$  could vary with time as well.

The equation of motion for the  $2\pi$  kink is then found, using the expression for the momentum for a soliton solution to the unperturbed sine-Gordon equation:

$$P_k = 8\gamma(v)v, \quad \gamma(v) = (1 - v^2)^{-1/2} \quad (2.8)$$

where  $v$  is the velocity of the  $2\pi$  kink. With this assumption [Eq. (2.8)] Eq. (2.6) becomes the relativistic version of Newton's second law for a  $2\pi$  kink with a friction term, a force term, and terms

representing interaction between the  $2\pi$  kink and the background yielding an acceleration  $a$ , given by

$$[\gamma(v)]^3 a = -\frac{1}{4}\pi \sin[\phi^{\text{vac}}(t)] - \alpha\gamma(v)v. \quad (2.9)$$

From Eq. (2.9) the importance of the initial state of vacuum is obvious. If the vacuum is in its ground state  $\phi^{\text{vac}} = -\sin^{-1}\eta$  [the trivial solution to Eq. (2.3)], the force term becomes  $2\pi\eta$ , yielding an initial acceleration  $a_i$ :

$$a_i = \frac{1}{4}\pi\eta. \quad (2.10)$$

On the other hand, if the vacuum was started with  $\phi^{\text{vac}}(0) = 0$  and  $\phi_t^{\text{vac}}(0) = 0$ , Eq. (2.9) yields an initial acceleration<sup>1</sup>

$$a_i = \frac{1}{8}\pi\eta t^2, \quad (2.11)$$

which shows that the initial state of the vacuum in Ref. 1 forces the  $2\pi$  kink to start up very slowly. Other initial conditions of the vacuum would give other initial accelerations [Eq. (2.9)].

### Examples

In the following we solve Eq. (2.5) in order to obtain expressions for the velocity of the  $2\pi$  kink in two special cases: constant  $\eta$  and harmonic time-varying  $\eta$ . For *constant*  $\eta$  the solution of Eq. (2.5) using Eq. (2.4) yields

$$P_k = 2\pi\frac{\eta}{\alpha}(1 - e^{-\alpha t}) + 2\pi\phi_t^{\text{vac}}. \quad (2.12)$$

Expressions for  $\phi_t^{\text{vac}}$  can easily be found for  $\phi^{\text{vac}}(0) = -\sin^{-1}\eta$  and  $\phi_t^{\text{vac}}(0) = 0$ , and  $\phi^{\text{vac}}(0) = 0$  and  $\phi_t^{\text{vac}}(0) = 0$  by solving Eq. (2.3). In the latter case we assume  $\eta \ll 1$  such that  $\phi^{\text{vac}}(t) \ll 1$  in order to linearize Eq. (2.3) to obtain analytic expressions. The solution [Eq. (2.12)] can then be written

$$P_k = \frac{2\pi\eta}{\alpha}(1 - e^{-\alpha t}) \quad (2.13a)$$

or

$$\begin{aligned} P_k &= 2\pi\eta \left[ \frac{\sinh(\alpha t/2)}{\alpha/2} - \frac{\sin[1 - (\alpha/2)^2]^{1/2} t}{[1 - (\alpha/2)^2]^{1/2}} \right] e^{-\alpha t/2}. \end{aligned} \quad (2.13b)$$

In (2.13a)  $\phi^{\text{vac}}$  is in the ground state while in (2.13b)  $\phi^{\text{vac}}$  is in the excited state  $\phi^{\text{vac}}(0) = 0$ .

Solving Eq. (2.8) with respect to  $v$  yields

$$v = \frac{P_k}{(64 + P_k^2)^{1/2}}. \quad (2.14)$$

This equation represents an ordinary differential

equation determining the trajectory of the  $2\pi$  kink ( $v = dx/dt$ ). This equation can be solved analytically for  $P_k$  given by Eq. (2.13a).<sup>6</sup>

Finally, we stress that the analysis also is valid for  $\eta = \eta(t)$ . As simple examples we choose (a)  $\eta = \eta_0 \sin(\omega t)$ ,  $\phi^{\text{vac}}(0) = \phi_t^{\text{vac}}(0) = 0$ , and  $\alpha = 0$  and (b)  $\eta = \eta_0 \cos(\omega t)$ ,  $\phi^{\text{vac}}(0) = \phi_t^{\text{vac}}(0) = 0$ , and  $\alpha = 0$ . For  $\eta \ll 1$  or  $\omega \gg 1$  we get from Eq. (2.6) (assuming  $|\omega| \neq 1$ ) for case (a):

$$\gamma(v)v = \frac{\pi\eta_0}{4\omega} + \frac{\pi\eta_0}{4} \frac{1}{\omega^2 - 1} \left[ \frac{\cos(\omega t)}{\omega} - \omega \cos t \right], \quad (2.15)$$

which gives an approximate expression for the velocity  $v(t)$ . For  $v \ll 1$ , integration of (2.15) yields the trajectory of the  $2\pi$  kink:

$$x = x_0 + \frac{\pi\eta_0}{\omega} t + \frac{\pi\eta_0}{4} \frac{1}{\omega^2 - 1} \left[ \frac{\sin(\omega t)}{\omega^2} - \omega \sin t \right]. \quad (2.16)$$

Here  $x_0 = x(0)$  is the initial location of the  $2\pi$  kink. In case (b) we get

$$\gamma(v)v = -\frac{\pi\eta_0}{4} \frac{1}{\omega^2 - 1} \left[ \frac{\sin(\omega t)}{\omega} - \sin t \right], \quad (2.17)$$

which for  $v \ll 1$  can be integrated to give the trajectory of the  $2\pi$  kink:

$$x = x_0 + \frac{\pi\eta_0}{4\omega^2} + \frac{\pi\eta_0}{4} \frac{1}{\omega^2 - 1} \left[ \frac{\cos(\omega t)}{\omega^2} - \cos t \right]. \quad (2.18)$$

Similar results can be obtained for  $\alpha \neq 0$ . We note the different behavior of the  $2\pi$  kink in cases (a) and (b). Although the  $2\pi$  kink oscillates in both cases, it travels to the right in case a.

In the next section we solve some representative initial-value problems numerically that illustrate the behavior of the  $2\pi$  kink in various situations.

### III. NUMERICAL INVESTIGATION OF INFLUENCE OF FORCE AND LOSS TERMS

In the preceding section we used a perturbation approach to derive the time evolution of the momentum. Application of the expression for the momentum of the exact  $2\pi$ -kink solution to the unperturbed sine-Gordon equation [Eq. (2.1) with  $\alpha = \eta = 0$ ] then yields expressions for the velocities when the vacuum is initially in the excited and

ground states. These expressions then give first-order differential equations that can be solved exactly in the latter case and approximately in the former case. In this section we show results of numerical solution of some representative initial-value problems.

We solve the initial-value problem equation (2.1) with

$$\begin{aligned} \phi(x, 0) &= 4 \tan^{-1}[\exp(x - x_0)] + (n - 1) \sin^{-1} \eta, \\ \phi_t(x, 0) &= 0, \\ \phi_x(0, t) &= \phi_x(l, t) = 0. \end{aligned} \quad (3.1)$$

Here the first term in  $\phi(x, 0)$  represents a static  $2\pi$  kink initially placed at  $x_0$ , while the second term for  $n = 1$  and  $n = 0$  gives the vacuum in the excited and ground states, respectively. The boundary conditions at  $x = 0$  and  $x = l$  represent lossless terminations.

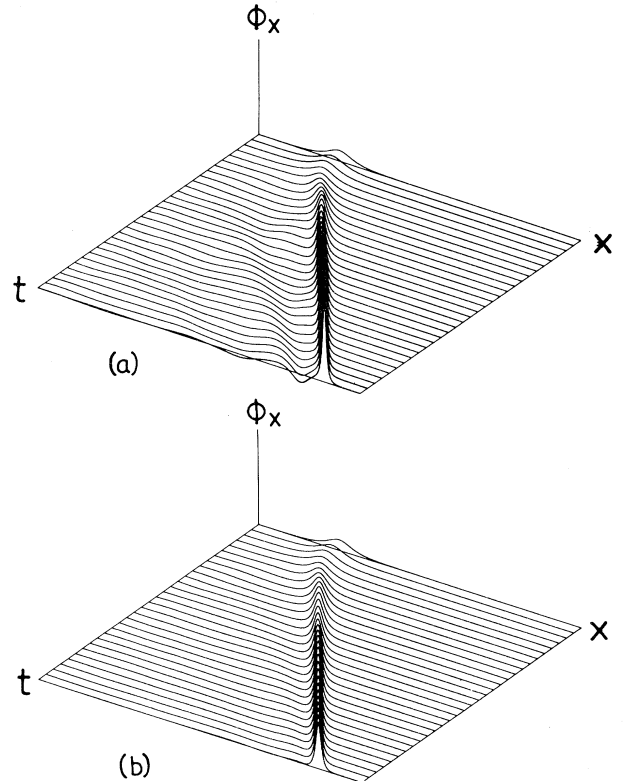


FIG. 1. Propagation of a  $2\pi$  kink under the influence of a force term and various values of the loss coefficient. The parameter values are  $\eta = 0.6$ ,  $n = 1$ , and  $\alpha = 0$  (a),  $\alpha = 0.1$  (b). The results are displayed in terms of  $\phi_x$  for  $0 \leq x \leq 30$  and  $0 \leq t \leq 21$ . The vacuum is initially in an excited state ( $n = 1$ ). In (a) the initially static  $2\pi$  kink is accelerated towards a Heaviside step function of velocity unity. In (b) the  $2\pi$  kink enters a motion with a stationary velocity determined by the balance between the external force and the loss.

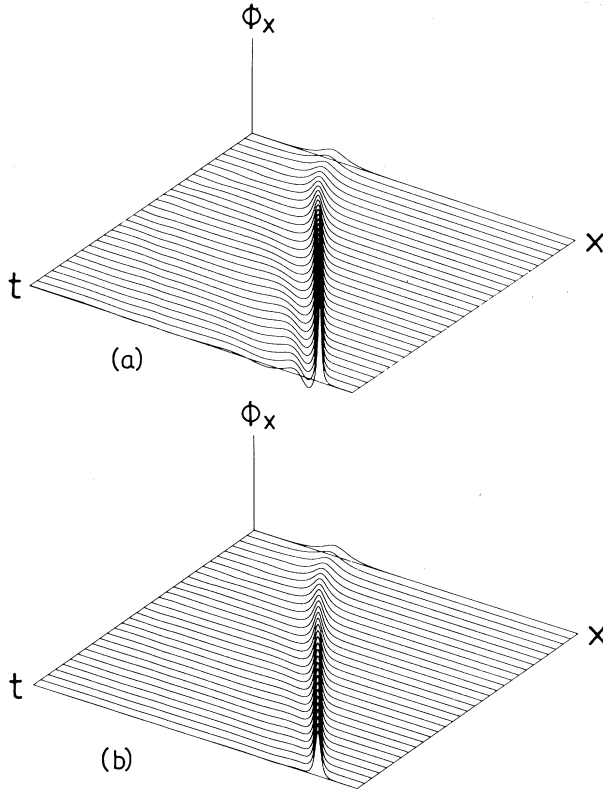


FIG. 2. Parameter values as in Fig. 1 except  $n=0$ . Thus the vacuum is in the ground state for  $t=0$ . Compared to Fig. 1 only minor differences in the time evolution of the  $2\pi$  kink are observed. However, for small values of  $t$  differences in acceleration, velocity and position of the  $2\pi$  kinks are found in accordance with the perturbation theory.

The numerical results are obtained by means of a computer program based on the method of characteristics and are displayed in terms of the derivative  $\phi_x(x, t)$ . Note that the maximum value of  $\phi_x$  for  $t=0$  is always equal to 2.

#### A. Influence of a constant-force term

In this section we present numerical solutions of the initial-value problem (2.1) with (3.1),  $\eta$  being constant. Throughout this section  $x_0=7.5$ .

In Fig. 1 we show how an initially static  $2\pi$  kink is influenced by a force term and various loss terms represented by different values of the loss parameter  $\alpha$ . The parameter values in Eq. (3.1) are  $0 \leq t \leq 21$ ,  $l=30$ ,  $\eta=0.6$ ,  $n=1$ , and  $\alpha=0$  [Fig. 1(a)],  $\alpha=0.1$  [Fig. 1(b)], i.e., the vacuum is initially in an excited state. In Fig. 1(a) the  $2\pi$  kink is accelerated towards a Heaviside step function (with a step of  $2\pi$ ) with a velocity approaching unity. The  $2\pi$  kink starts up slowly, but accelerates suddenly. At the same time a

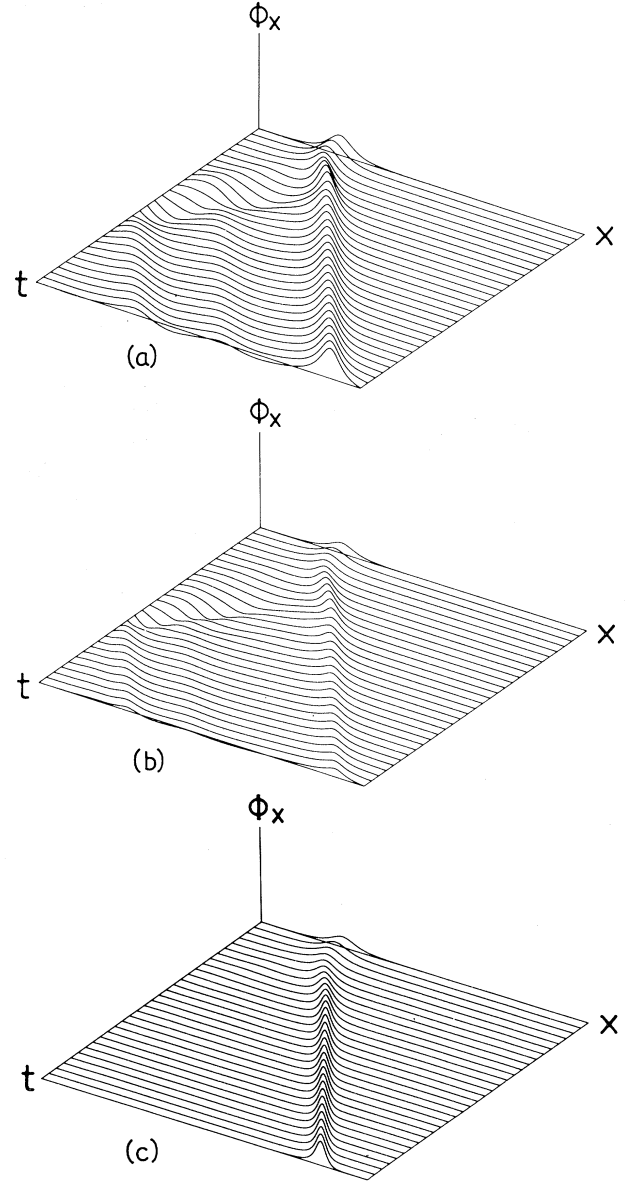


FIG. 3. Propagation of a  $2\pi$  kink under the influence of a force term above the critical value ( $\eta_c \sim 0.72461$ ) and various values of the loss coefficient. The parameter values in (2.1) and (3.1) are  $\eta=0.8$ ,  $n=1$ , and  $\alpha=0$  (a),  $\alpha=0.1$  (b),  $\alpha=0.3$  (c). The results are displayed in terms of the derivative  $\phi_x$  for  $0 \leq x \leq 30$  and  $0 \leq t \leq 21$ . The vacuum is initially in an excited state ( $n=1$ ). In (a) the initially static  $2\pi$  kink is accelerated to the right; the velocity approaches unity. Note that when the velocity equals unity, the Lorentz contraction stops. In this case the phase decreases monotonously. In (b) the same qualitative behavior is found even in the presence of loss. In (c) the loss coefficient has been enlarged compared to (b), and as a consequence the phase does not decrease monotonously and the  $2\pi$  kink enters a motion with a stationary velocity. Note the change in scale between part (a) and parts (b) and (c).

wake is seen to develop. Figure 1(b) shows the influence of a loss term. In accordance with the perturbation theory (and our physical intuition) the  $2\pi$  kink enters a motion with a stationary velocity determined by a balance between the force (energy input) and the loss (energy dissipation). The presence of the loss term prevents the wake to develop.

In Fig. 2 we show the time evolution of a  $2\pi$  kink that initially is static and when the vacuum is in the ground state [i.e.,  $n=0$  in Eq. (3.1)]. Except for  $n$ , the parameter values are the same as those in Fig. 1. Compared to Fig. 1, only minor differences are observed for large values of time ( $t \gtrsim 5$ ), while for small times differences in acceleration, velocity, and position of the  $2\pi$  kink are found in accordance with the perturbation theory in the preceding section. For smaller values of  $\alpha$  and  $\eta$  the same qualitative behavior is found. In the next section we perform a detailed comparison between velocities obtained numerically and from the perturbation theory for the

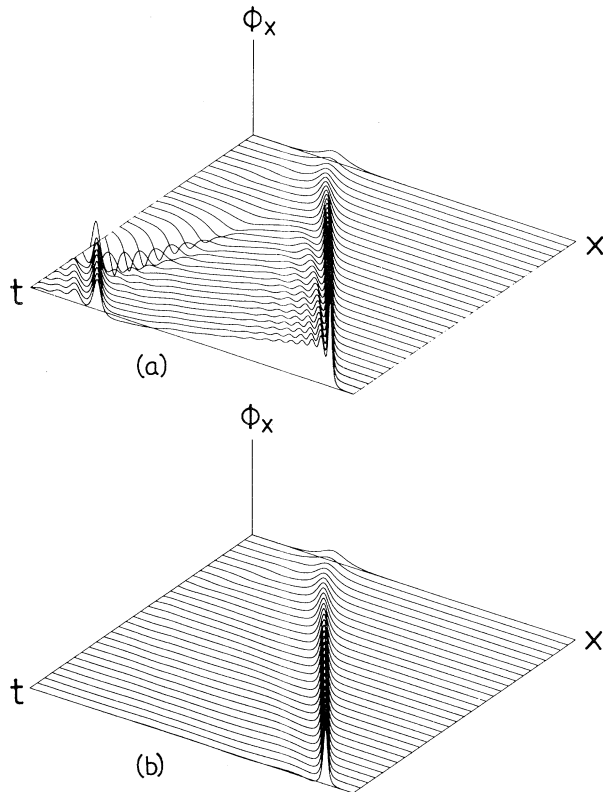


FIG. 4. Parameter values as in Fig. 3 except  $n=0$ . Thus the vacuum is in the ground state for  $t=0$ . In (a) [ $\alpha=0$  in (2.1)] the radiation emitted from the  $2\pi$  kink dissociates into a  $2\pi$  kink (traveling to the right) and a  $2\pi$  antikink (traveling to the left). After the dissociation the phase to the left of the leading  $2\pi$  kink starts decreasing, each ripple corresponding to a  $2\pi$  kink. This effect disappears in (b) ( $\alpha=0.1$ ), and the  $2\pi$  kink enters a stationary motion.

vacuum in the excited and the ground states, respectively.

The influence of an external force larger than the critical value ( $\eta_c=0.72461\dots$ ) given by Inoue and Chung<sup>8</sup> is shown in Figs. 3 and 4. For values of  $\eta$  larger than  $\eta_c$  they found that  $\phi$  starts decreasing monotonously [corresponding to rotating pendulums, Eq. (2.3)]. This occurs for  $\phi^{\text{vac}}(0)=0$  and  $\alpha=0$ .

In Fig. 3 the parameter values in (2.1) and (3.1) are  $0 \leq t \leq 21$ ,  $l=30$ ,  $\eta=0.8$ ,  $n=1$ , and  $\alpha=0$  [Fig. 3(a)],  $\alpha=0.1$  [Fig. 3(b)],  $\alpha=0.3$  [Fig. 3(c)]. Thus the  $2\pi$  kink is initially static and the vacuum in an excited state. The  $2\pi$  kink is accelerated to the right, while the phase  $\phi$  starts decreasing almost proportionally to  $-t^2$  [ $\phi(0,0)=0$ , and  $\phi(0,t)$  becomes  $-100$  for  $t=18.5$ ]. After emission of radiation the  $2\pi$  kink enters a stationary motion at a velocity equal to unity. The Lorentz contraction stops when the stationary velocity is reached. Furthermore, the maximum value of the derivative  $\phi_x$  oscillates with a period that is proportional to  $t^{-2}$ . This cannot be seen in Fig. 3(a) because of the scale. Thus the effect of an external force larger than  $\eta_c$  is that the phase starts decreasing, the  $2\pi$  kink approaches a velocity equal to unity, and the Lorentz contraction only takes place while the  $2\pi$  kink accelerates, i.e., there is no coupling between the Lorentz factor [as indicated in (2.8)] and the velocity. In Figs. 3(b) and 3(c) the influence of damping is shown [note the change in scale between Fig. 3(a) and Figs. 3(b) and 3(c)]. In Fig. 3(b) the same qualitative behavior is found even in the presence of loss ( $\alpha=0.1$ ); the phase decreases and the coupling between the Lorentz factor and the velocity does not occur. In Fig. 3(b), however, the loss ( $\alpha=0.3$ ) prevents the phase to decrease, and the  $2\pi$

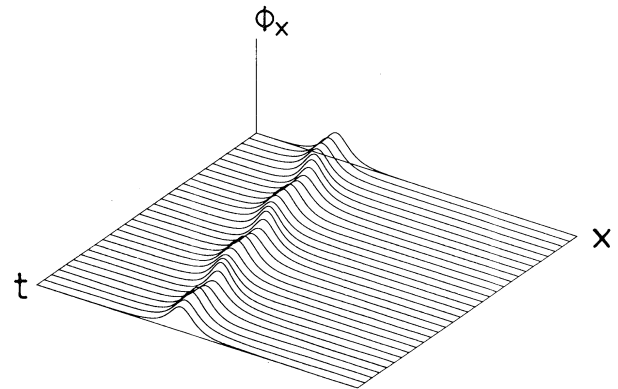


FIG. 5. Propagation of a  $2\pi$  kink under the influence of a time-dependent force,  $\eta=\eta_0 \sin(\omega t)$ . Parameter values in (2.1) and (3.1) are  $\eta_0=0.1$ ,  $\omega=0.5$ ,  $n=1$ , and  $\alpha=0$ . Although the  $2\pi$  kink oscillates it travels to the right.

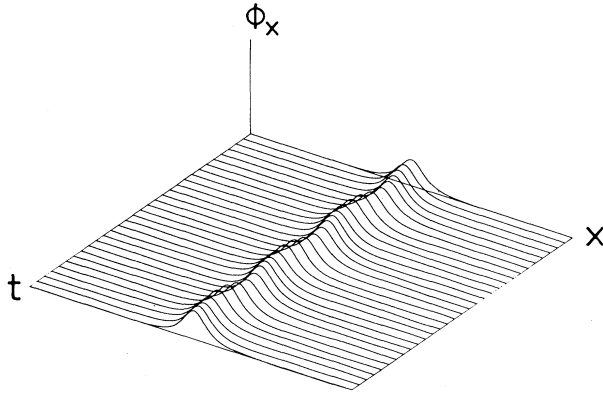


FIG. 6. Propagation of a  $2\pi$  kink under the influence of a time-dependent force,  $\eta = \eta_0 \cos(\omega t)$ . Parameter values as in Fig. 5. As a result of the force, the  $2\pi$  kink oscillates.

kink enters a stationary motion where the relation (2.8) between the Lorentz factor and the velocity holds.

In Fig. 4 we show the time evolution of a  $2\pi$  kink that initially is static and in the ground state [ $n=0$  in Eq. (3.1)]. The parameter values are the same as those in Fig. 3. In Fig. 4(a) ( $\alpha=0$ ) the radiation emitted from the  $2\pi$  kink dissociates into a  $2\pi$  kink (traveling to the right) and a  $2\pi$  antikink (traveling

to the left), which after reflection at  $x=0$  starts a train of  $2\pi$  kinks. After the dissociation the phase to the left of the leading  $2\pi$  kink starts decreasing monotonously, each ripple corresponding to a  $2\pi$  kink. This effect has also been observed for  $n=1$ ,  $\alpha=0$ , and  $\eta=0.7$ . In Fig. 4(b) ( $\alpha=0.1$ ) the effect disappears because of the loss term.

### B. Influence of a time-dependent force

In this section we examine the two examples of time-dependent forces proposed in Sec. II. Thus we solve the initial-value problem (2.1) and (3.1) with  $0 \leq t \leq 42$ ,  $l=30$ ,  $n=1$ ,  $\alpha=0$ ,  $\eta = \eta_0 \sin(\omega t)$ ,  $\eta_0=0.1$ , and  $\omega=0.5$ . In Fig. 5 the results are displayed in terms of  $\phi_x$ . In agreement with the analysis in Sec. II the  $2\pi$  kink travels to the right while it oscillates.

In Fig. 6 we have shown the results when the time-dependent force is chosen as case (b) in Sec. II. The parameter values in (2.1) and (3.1) are  $0 \leq t \leq 42$ ,  $l=30$ ,  $n=1$ ,  $\alpha=0$ ,  $\eta = \eta_0 \cos(\omega t)$ ,  $\eta_0=0.1$ , and  $\omega=0.5$ . In this case the  $2\pi$  kink oscillates in accordance with the analysis in Sec. II. In the next section a comparison is made between the numerical results and the analysis.

## IV. COMPARISONS BETWEEN NUMERICAL RESULTS AND ANALYSIS

In this section we present some comparisons between numerical results and the theory. The numerically determined velocity is calculated from the formula

$$v(t) = - \frac{\phi_{t,\max} - \phi_t^{\text{vac}}(t)}{\phi_{x,\max}}, \quad (4.1)$$

where  $\phi_{t,\max}$  and  $\phi_{x,\max}$  are the values of  $\phi_t$  and  $\phi_x$  at the time  $t$  at the point where the derivative  $\phi_x$  of the  $2\pi$  kink has the maximum. The second term in the numerator eliminates the vacuum part of  $\phi$  [Eq. (2.2)]. The advantage of using Eq. (4.1) instead of measuring the velocity of the center of mass of the  $2\pi$  kink<sup>1</sup> is that the radiation that is created as a result of the acceleration influences the center-of-mass calculation of the  $2\pi$  kink and thus introduces an error in the estimate of the velocity. We find a difference of less than 10% between the velocities determined by the two methods for  $t \lesssim 3$  while for larger times large differences occur.

### A. Constant-force and loss terms

In Fig. 7 we have shown the velocity  $v(t)$  as a function of time  $t$  in the case where the vacuum is initially in the ground state [Fig. 7(a)] and in the case where the vacuum is initially in an excited state

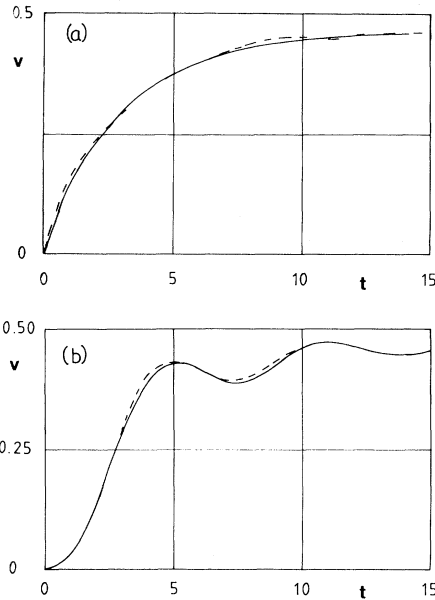


FIG. 7. Comparison between results obtained from the perturbation analysis and numerical experiments for  $\eta=0.2$  and  $\alpha=0.3$ . In (a) the vacuum is in the ground state, while in (b) the vacuum is in an excited state. Solid curves are given by Eq. (2.14) with (2.13). The numerically determined velocities are given by the dashed curves. Good agreement between analysis and numerical results is found.

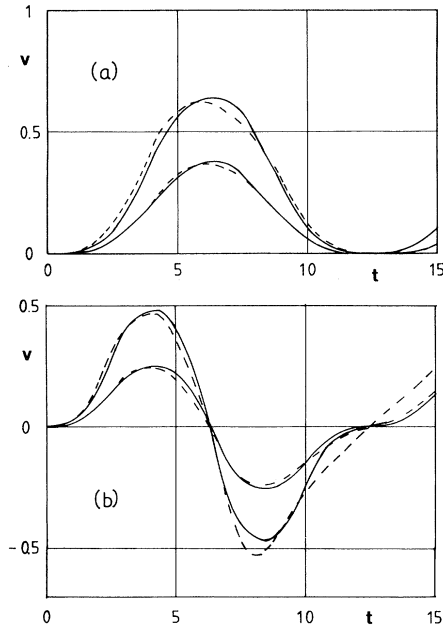


FIG. 8. Comparison between velocities obtained from the analysis and from numerical computations in the case of a time-dependent force. In (a)  $\eta(t) = \eta_0 \sin(\omega t)$ ,  $\omega = 0.5$ , and  $\eta_0 = 0.1$  (lower curves),  $\eta_0 = 0.2$  (upper curves). Solid curves are found from the perturbation theory; dashed curves are numerically determined. In (b)  $\eta(t) = \eta_0 \cos(\omega t)$ ,  $\omega = 0.5$ , and  $\eta_0 = 0.1$  (lower curves),  $\eta_0 = 0.2$  (upper curves).

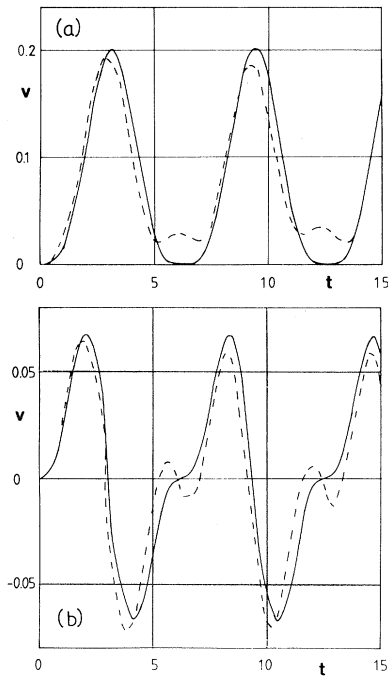


FIG. 9. In (a)  $\eta(t) = \eta_0 \sin(\omega t)$ ,  $\eta_0 = 0.2$ , and  $\omega = 2$ , while in (b)  $\eta(t) = \eta_0 \cos(\omega t)$ ,  $\eta_0 = 0.2$ , and  $\omega = 2$ . Solid curves represent the analysis; dashed curves are numerically determined.

[Fig. 7(b)]. The parameter values in (2.1) are in both cases  $\eta = 0.2$  and  $\alpha = 0.3$  while in (3.1)  $n = 0$  [Fig. 7(a)] and  $n = 1$  [Fig. 7(b)]. In Fig. 7(a) the velocity is seen initially to increase proportional to time, i.e., it exhibits a Newtonian behavior. For  $t \rightarrow \infty$  the velocity is seen to approach the stationary velocity  $v_\infty$  (which represents a balance between energy input and energy dissipation). The stationary velocity can be found from Eq. (2.5) by inserting  $P = 8v_\infty \gamma(v_\infty)$ . The solid curve in Fig. 7(a) is given by Eq. (2.14) with Eq. (2.13a) inserted. The dashed curve shows the velocity obtained numerically. Good agreement between analysis and numerical results is observed. For smaller values of the parameters  $\alpha$  and  $\eta$  a similar agreement is found. Figure 7(b) shows the comparison for the vacuum initially in an excited state. The solid curve is given by Eq. (2.14) with Eq. (2.13b), and the dashed curve shows the velocity obtained numerically. Initially, the velocity of the  $2\pi$  kink starts up proportional to  $t^3$ . For  $t \rightarrow \infty$  the velocity tends towards  $v_\infty$ . Again, good agreement is found between the analysis and the numerical results.

### B. Time-varying force

In this section we show comparisons between the velocity determined from the analysis and from numerical solutions in the case of time-dependent forces,  $\eta(t) = \eta_0 \sin(\omega t)$  or  $\eta(t) = \eta_0 \cos(\omega t)$ . In Fig. 8 the frequency  $\omega$  is smaller than unity. The solid curves are given by (2.15) [Fig. 8(a)] and (2.17) [Fig. 8(b)], respectively. The dashed curves are obtained numerically. Good agreement is observed between the results obtained analytically and numerically.

Figure 9 shows the velocity as a function of time in the case of  $\omega > 1$ . In Fig. 9(a)  $\eta = \eta_0 \sin(\omega t)$ ,  $\eta_0 = 0.2$ , and  $\omega = 2$ , while in Fig. 9(b)  $\eta = \eta_0 \cos(\omega t)$ ,  $\eta_0 = 0.2$ , and  $\omega = 2$ . The agreement between the analysis is good for  $v \neq 0$  but fails in the vicinity of  $v = 0$ .

## V. CONCLUSION

In this paper we have examined the influence of external force and dissipation on a  $2\pi$ -kink solution to a perturbed sine-Gordon equation. The behavior of the  $2\pi$  kink depends strongly on the initial state of the vacuum. This is explained by a simple analysis based on the approach that the solution to the problem can be divided into a vacuum part and a  $2\pi$ -kink part. Approximate expressions for the velocity of the  $2\pi$  kink are given in the cases of constant and time-varying forces and compared with the velocity obtained by numerical solution of some representative initial-value problems. Good agreement is found for  $\eta, \alpha \ll 1$  (for large values of these



parameters one must solve the pendulum equation numerically). However, for small times we find a remarkably good agreement even for larger  $\eta$  and  $\alpha$ . This can be understood from Eq. (2.7), which shows that as long as  $P_k$  and  $\phi^{\text{vac}}$  are small the perturbation is small.

Finally we note that the analysis in this paper

does not explicitly take the  $k \neq 0$  part of the possible radiation into account; we only consider the coupling between the  $2\pi$  kink and the vacuum, which contains the  $k = 0$  part of the radiation. The  $k \neq 0$  part of the radiation is very difficult to calculate; this has only been done in Ref. 1 and elsewhere recently<sup>9</sup> for  $\phi^{\text{vac}}(0) = a \ll 2\pi$ ,  $\phi_t^{\text{vac}}(0) = 0$ .

---

<sup>1</sup>J. C. Fernandez, M. J. Gambaudo, S. Gauthier, and G. Reinisch, Phys. Rev. Lett. **46**, 753 (1981); G. Reinisch and J. C. Fernandez, Phys. Rev. B **24**, 835 (1981).

<sup>2</sup>M. B. Fogel, S. E. Trullinger, A. R. Bishop, and J. A. Krumhansl, Phys. Rev. Lett. **36**, 1411 (1976); **37**, 314 (1976); M. B. Fogel, S. E. Trullinger, A. R. Bishop, and J. A. Krumhansl, Phys. Rev. B **15**, 1578 (1977).

<sup>3</sup>D. W. McLaughlin and A. C. Scott, Phys. Rev. A **18**, 1652 (1978).

<sup>4</sup>O. H. Olsen and M. R. Samuelsen, Phys. Rev. Lett. **48**, 1569 (1982).

<sup>5</sup>O. H. Olsen and M. R. Samuelsen, Phys. Scr. **23**, 1033 (1981).

<sup>6</sup>O. H. Olsen and M. R. Samuelsen, Phys. Rev. B **25**, 3181 (1982).

<sup>7</sup>E. Joergensen, V. P. Koshelets, R. Monaco, J. Mygind, M. R. Samuelsen, and M. Salerno, Phys. Rev. Lett. **49**, 1093 (1982).

<sup>8</sup>M. Inoue and S. G. Chung, J. Phys. Soc. Jpn. **46**, 1594 (1979).

<sup>9</sup>G. Reinisch and J. C. Fernandez, Phys. Rev. B **25**, 7352 (1982).